Eur Biophys J (1989) 17:101–111

European Biophysics Journal

Membrane bending energy and shape determination of phospholipid vesicles and red blood cells

S. Svetina * and B. Žekš

Institute of Biophysics, Medical Faculty, Lipičeva 2, and J. Stefan Institute, E. Kardelj University of Ljubljana, YU-61105 Ljubljana, Yugoslavia

Received October 7, 1988/Accepted in revised form February 8, 1989

Abstract. A procedure is developed to calculate red blood cell and phospholipid vesicle shapes within the bilayer couple model of the membrane. The membrane is assumed to consist of two laterally incompressible leaflets which are in close contact but unconnected. Shapes are determined by minimizing the membrane bending energy at a given volume of a cell (V), given average membrane area (A) and given difference of the areas of two leaflets (ΔA). Different classes of shapes exist in parts of the $v/\Delta a$ phase diagram, where v and Δa are the volume and the leaflet area difference relative to the sphere with area A. The limiting shapes are composed of sections of spheres with only two values allowed for their radii. Two low energy axisymmetrical classes, which include discocyte and stomatocyte shapes are studied and their phase diagrams are analyzed. For $v = 0.6$, the discocyte is the lowest energy shape, which transforms by decreasing Δa continuously into a stomatocyte. The spontaneous membrane curvature (C_0) and compressibility of membrane leaflets can be incorporated into the model.

A model, where ΔA is free and C_0 determines the shapes at given V and A, is also studied. In this case, by decreasing C_0, a discocyte transforms discontinuously into an almost closed stomatocyte.

Key words: Phospholipid membrane, red blood cell shapes, membrane bending energy

Introduction

The inner solutions of red blood cells (RBC) and phospholipid vesicles (PV) do not involve any structure and therefore the shapes of these objects depend solely on the physical and chemical state of their membranes. It is commonly believed that for a given membrane the shapes that are formed correspond to the minimum value of the membrane elastic energy. This energy can, in general, be decomposed into the sum of the stretching, shear and bending energy terms (Evans and Skalak 1980). It is also a general property of membranes that relatively much more energy is needed to stretch them than to cause shear deformation or bending. Consequently, the shape established by a flaccid cell or vesicle corresponds to the minimum value of the sum of the shear and bending energy terms, where its membrane area is practically constant. In particular, phospholipid membranes are two-dimensional liquids and as such do not exhibit shear elasticity. Thus their shape is determined only by the membrane bending energy. The RBC membrane is structurally more complex than the PV membrane, involving, for example, a cytoplasmic protein network. The RBC membrane exhibits shear elasticity (Hochmuth and Waugh 1987) and how this may affect the cell shape has been theoretically analyzed (Zarda et al. 1977). However, which of the above two elastic deformations is the main determinant of the RBC shape still cannot be definitely established. At least some of the shapes observed in PV and RBC systems are alike (Sackmann et al. 1986), which indicates a possible dominant role of the membrane bending energy. It is therefore of interest to investigate the RBC shape behavior under the assumption of a minimum value of membrane bending energy as a possible limiting case of a more general situation.

The idea that the RBC shape is determined by the minimum value of the total membrane bending energy has been introduced by Canham (1970) who, by approximating the RBC geometry by the ovals of Cassini, obtained theoretically that at constant cell volume and membrane area, the shape with the minimum value of membrane bending energy is a discocyte. Jenkins (1977), by applying a general variational principle to the problem of shape determination, has

* To whom offprint requests should be sent

shown that at a given cell volume there is a multiplicity of possible axisymmetrical shapes, in which some involve equatorial reflection symmetry (symmetrical shapes), and others do not (asymmetrical shapes). Helfrich and Deuling (1975) extended the minimum bending energy approach by also taking into consideration the spontaneous curvature, the membrane material property measuring the asymmetry of the membrane. By comparing the calculated bending energies of two classes of symmetrical axisymmetrical shapes, oblate and prolate, they concluded that the oblate shape which at lower volumes gives rise to discocyte shapes, has at a given larger volume a smaller value of membrane bending energy only if the spontaneous curvature is sufficiently negative. In a continuation of their work, Deuling and Helfrich (1976a) gave a catalogue of vesicle shapes, the shapes having been calculated at different values of enclosed volume, membrane area and spontaneous curvature. A large variety of axisymmetrical shapes was presented, allowing for indentations, cavities and contact of the membrane with itself. Deuling and Helfrich (1976b) have also shown the similarity of some calculated shapes with discocyte and stomatocyte RBC shapes. Luke (1982) contributed an efficient numerical method for calculating vesicle shapes and presented some more shapes, in particular some appearing at positive values of spontaneous curvature, which suggests a vesicle cleavage phenomenon (Luke and Kaplan 1979). More recently Peterson (1985) performed a stability analysis of vesicle shapes which indicated that, for a given cell or vesicle volume, the axisymmetrical shapes are not stable at all values of spontaneous curvature.

Another line of RBC shape research has indicated the importance of the fact that the RBC membrane is composed of layers. Evans (1974), when treating the mechanical properties of layered membranes, introduced the concept of chemically induced average curvature. The notion of this membrane property is very clearly represented in qualitative terms by the bilayer couple hypothesis (Sheetz and Singer 1974). In its most general form, this hypothesis is that the two leaflets of the closed membrane bilayer may respond differently to various perturbations while remaining in contact. The bilayer couple hypothesis was introduced in order to provide a qualitative explanation for RBC shape transformations which arise because of the interaction of the RBC membrane with a wide range of amphipathic molecules. Those of them which bind preferentially to the cytoplasmic side of the membrane were assumed to expand the inner bilayer leaflet relative to the outer, thus causing a cell to convert from the normal biconcave disc shape (discocyte) to a cupped form (stomatocyte). Those amphipathic compounds which bind preferentially to the external half of the bilayer, were assumed to expand the outer leaflet relative to the inner one, thus causing a normal cell to convert into a crenated form (an echinocyte). Because the cytoplasmic side of the bilayer part of the RBC membrane is highly negative and the external side is practically neutral, the above conclusions accord with the observation of Deuticke (1968) that most of the compounds which crenate the RBC are anionic amphipathic and that most of the cup formers are cationic amphipathic.

The idea of coupled layers can be incorporated into the quantitative treatment of RBC and PV shapes based on the membrane bending energy by considering in the minimization procedure, in addition to the constancy of the cell volume and the membrane area, the constraint of the constancy of the difference between the areas of the two bilayer leaflets (Svetina et al. 1982). The application of a strict variational approach to the problem (Svetina and Žekš 1983, 1984, 1985) has indicated a number of interesting properties of this system, such as the occurrence of symmetry instabilities and geometrical limitations of possible shapes. The aim of this work is to give a more thorough presentation of these properties.

In the first part, the theoretical procedure for the determination of axisymmetrical shapes of bilayered vesicles and cells is presented. Particular emphasis is devoted to the determination of limiting shapes due to geometrical restrictions. Properties of the system are then discussed by treating two representative classes of shapes, the class of symmetrical shapes which includes the discocyte shapes and the class of asymmetrical shapes which includes the cup (stomatocyte) shapes. The corresponding analysis is first worked out for the case of no spontaneous curvature, which allows those properties of the system treated which do not depend on the material constants of the membrane to be singled out. The effect of the inclusion of the spontaneous curvature is discussed separately.

Theory

(i) Minimization of the membrane bending energy

The problem is to find the extreme values of the membrane bending energy

$$W_b = \tfrac{1}{2} K \int (C_1 + C_2)^2 \, \mathrm{d}A^*, \tag{1}$$

where K is the membrane bending elastic constant, C_1 and C_2 are the two principal curvatures, and integration is performed over the whole area of the neutral surface of the bilayer (A^*). The minimization procedure is to be carried out at fixed values of cell volume (V), area of neutral surface (A) and difference between the areas of the two membrane leaflets (ΔA).

The shape of a cell can therefore be obtained by minimizing the functional[1]

$$G = W_b - \lambda(A^* - A) - \mu(V^* - V) - \nu(\Delta A^* - \Delta A). \quad (2)$$

Where A^*, V^* and ΔA^* are the membrane area, cell volume and the difference in leaflet areas, respectively, and the three Lagrange multipliers (λ, μ, ν) are determined from the conditions

$$A^* = A, \quad V^* = V, \quad \Delta A^* = \Delta A. \quad (3)$$

The difference in leaflet areas

$$\Delta A^* = \delta \int (C_1 + C_2)\, \mathrm{d}A^* \quad (4)$$

is proportional to the average curvature. Here δ is the distance between the neutral surfaces of the two leaflets.

The expression for the membrane bending energy (Eq. 1) is scale invariant, i.e. it has the property that for a given shape it does not depend on the cell or vesicle size. It is therefore appropriate in the forthcoming analysis to choose the unit of length in such a way that the membrane area equals unity. If R_s is the radius of the sphere with the membrane area A

$$R_s = (A/4\pi)^{1/2} \quad (5)$$

the new variables, i.e. the two dimensionless curvatures, are

$$c_1 = R_s C_1, \quad c_2 = R_s C_2. \quad (6)$$

It is then also convenient to define the relative volume

$$v = V/V_s, \quad V_s = 4\pi R_s^3/3 \quad (7)$$

and relative difference between the areas of the two membrane leaflets

$$\Delta a = \Delta A/\Delta A_s, \quad \Delta A_s = 8\pi\delta R_s \quad (8)$$

while relative area $a = 1$. In an analogous manner, the relative area element can be expressed as

$$\mathrm{d}a^* = \mathrm{d}A^*/4\pi R_s^2 \quad (9)$$

and $v^* = V^*/V_s$, $\Delta a^* = \Delta A^*/\Delta A_s$.

It is clear that the result of the minimization procedure does not depend on the value of the membrane bending constant, K. It is therefore appropriate to measure also the membrane bending energy and the energy functional G (Eq. 2) relative to the bending energy of the sphere

$$w_b = W_b/8\pi K, \quad g = G/8\pi K. \quad (10)$$

1 In Eq. (2) the Lagrange multiplier λ, which corresponds to the lateral tension in the membrane, is assumed to have the same value at all points of the membrane. A more general treatment shows, however, that the lateral tension changes over the contour and depends on the local curvature (Evans 1980). This dependence is proportional to the square of the curvature and in the present treatment is neglected.

We therefore obtain for the dimensionless energy functional g the expression

$$g = \tfrac{1}{4}\int (c_1 + c_2)^2\, \mathrm{d}a^* - \tfrac{1}{4}L(a^* - 1) - \tfrac{1}{6}M(v^* - v) - \tfrac{1}{2}N(\Delta a^* - \Delta a). \quad (11)$$

Here the new Lagrange multipliers L, M and N are related to λ, μ and ν as

$$L = \lambda \frac{2R_s^2}{K}, \quad M = \mu \frac{R_s^3}{K}, \quad N = \nu \frac{2\delta R_s}{K}. \quad (12)$$

It is easy to see from the structure of the energy functional G (Eq. 2) that the three Lagrange multipliers λ, μ and ν represent the thermodynamically conjugated fields to A, V and ΔA, respectively. Therefore, at equilibrium, when $W_b = W_b(A, V, \Delta A)$, the Lagrange multipliers are given by

$$\lambda = \frac{\partial W_b}{\partial A}, \quad \mu = \frac{\partial W_b}{\partial V}, \quad \nu = \frac{\partial W_b}{\partial \Delta A}. \quad (13)$$

On the other hand, one can conclude from Eq. (11) that at equilibrium, the bending energy $W_b = 8\pi K w_b(v, \Delta a)$ depends only on v and Δa. As a consequence, the Lagrange multipliers are interrelated as

$$A\lambda + \tfrac{3}{2}V\mu + \tfrac{1}{2}\Delta A\nu = 0 \quad (14)$$

or in the dimensionless form

$$L + vM + \Delta a N = 0. \quad (15)$$

Following the procedure used by Deuling and Helfrich (1976a), for a cell with an axisymmetrical shape, the corresponding contour $x = x(z)$, with z the dimensionless coordinate along the axis and x the dimensionless distance from the axis, can be obtained by minimizing the functional g (Eq. 11), which can be expressed for the axially symmetric case as

$$g = \tfrac{1}{4}\int (c_p + c_m)^2\, \mathrm{d}a^* - \tfrac{1}{4}L(a^* - 1) - \tfrac{1}{6}M(v^* - v) - \tfrac{1}{2}N(\Delta a^* - \Delta a). \quad (16)$$

Here c_p is the principal curvature along the parallels and c_m is the principal curvature along the meridians, and the geometrical parameters of the cell are given by

$$a^* = \tfrac{1}{2}\int \frac{x\, \mathrm{d}x}{[1 - (x c_p)^2]^{1/2}} \quad (17)$$

$$v^* = \tfrac{3}{4}\int \frac{x^3 c_p\, \mathrm{d}x}{[1 - (x c_p)^2]^{1/2}} \quad (18)$$

$$\Delta a^* = \tfrac{1}{4}\int \frac{(c_p + c_m)\, x\, \mathrm{d}x}{[1 - (x c_p)^2]^{1/2}}. \quad (19)$$

The two principal curvatures of an axisymmetrical object are interrelated

$$c_m = c_p + x \frac{\mathrm{d}c_p}{\mathrm{d}x} \quad (20)$$

and the above functional g can therefore be expressed as

$$g = \int \tilde{g}\left(x, c_p, \frac{\mathrm{d}c_p}{\mathrm{d}x}\right) \mathrm{d}x. \quad (21)$$

The variational procedure therefore leads to the Lagrange-Euler equation

$$\frac{\partial \tilde{g}}{\partial c_p} - \frac{\mathrm{d}}{\mathrm{d}x}\frac{\partial \tilde{g}}{\partial(\mathrm{d}c_p/\mathrm{d}x)} = 0 \tag{22}$$

which has a form of a second-order differential equation for $c_p(x)$:

$$\frac{x}{2(1-x^2c_p^2)}\left[x c_p \frac{\mathrm{d}c_p}{\mathrm{d}x}\left(2c_p + x\frac{\mathrm{d}c_p}{\mathrm{d}x}\right) + M + L c_p + N c_p^2\right] + \frac{\mathrm{d}}{\mathrm{d}x}\left(2c_p + x\frac{\mathrm{d}c_p}{\mathrm{d}x}\right) = 0. \tag{23}$$

The latter can be appropriatelly re-expressed as a system of two first order differential equations for $c_p(x)$ and $c_m(x)$

$$\frac{\mathrm{d}c_p}{\mathrm{d}x} = \frac{c_m - c_p}{x} \tag{24}$$

$$\frac{\mathrm{d}c_m}{\mathrm{d}x} = \frac{x}{2(1-x^2c_p^2)}[c_p(c_p^2 - c_m^2) - M - L c_p - N c_p^2] - \frac{c_m - c_p}{x}. \tag{25}$$

By introducing a new independent variable $f = x^2$ the equations read

$$\frac{\mathrm{d}c_p}{\mathrm{d}f} = \frac{c_m - c_p}{2f} \tag{26}$$

$$\frac{\mathrm{d}c_m}{\mathrm{d}f} = \frac{1}{4(1-f c_p^2)}[c_p(c_p^2 - c_m^2) - M - L c_p - N c_p^2] - \frac{c_m - c_p}{2f}. \tag{27}$$

The Lagrange multipliers M, N, L are determined by using the conditions $v^* = v$, $\Delta a^* = \Delta a$ and $a^* = 1$ where

$$v^* = \tfrac{3}{2}\int_0^1 f c_p \,\mathrm{d}a^* \tag{28}$$

$$\Delta a^* = \tfrac{1}{2}\int_0^1 (c_p + c_m)\,\mathrm{d}a^*, \tag{29}$$

where

$$\mathrm{d}a^* = \frac{\mathrm{d}f}{4(1-f c_p^2)^{1/2}} \tag{30}$$

while the relative energy of the cell is given by

$$w_b = \tfrac{1}{4}\int_0^1 (c_p + c_m)^2 \,\mathrm{d}a^* \tag{31}$$

The contour $f(z)$ is obtained by performing the integration

$$z = z_0 \mp \tfrac{1}{2}\int \frac{c_p \,\mathrm{d}f}{(1-f c_p^2)^{1/2}}, \tag{32}$$

where z_0 is the coordinate of a pole and the sign always changes when the extremum in the function $f(z)$ is reached.

In the numerical determinations of shapes it is necessary to pay special attention to the behavior of the system close to the extremes of the function $f(z)$ and to its zeros, i.e. to the poles of the axially symmetric shape. The requirement that the membrane surface at the poles is a continuous and derivable function gives rise to the following relationships

$$c_p(f=0) = c_m(f=0) \tag{33}$$

$$\left.\frac{\mathrm{d}c_p}{\mathrm{d}f}\right|_{f=0} = -\frac{1}{16}(N c_p^2 + L c_p + M) \tag{34}$$

$$\left.\frac{\mathrm{d}c_m}{\mathrm{d}f}\right|_{f=0} = -\frac{3}{16}(N c_p^2 + L c_p + M). \tag{35}$$

Each cell involves an odd number of extremes in the function $f(z)$. At these extremes, according to the definition of the curvature along the parallels it is

$$f^* c_p^{*2} = 1. \tag{36}$$

Also

$$c_p^*(c_p^{*2} - c_m^{*2}) - N c_p^{*2} - L c_p^* - M = 0. \tag{37}$$

The two curvatures in the surroundings of the these extremes can be expanded as

$$c_p = c_p^* - c_p'^* \varepsilon + \ldots \tag{38}$$

$$c_m = c_m^* - \alpha \varepsilon^{1/2} - \beta\varepsilon + \ldots, \tag{39}$$

where

$$\varepsilon = \pm(f^* - f) \tag{40}$$

with plus for maxima and minus for minima in the function $f(z)$. The first expansion coefficient in the expansion of c_p can be determined in terms of c_p^* and c_m^* as

$$c_p'^* = \pm\tfrac{1}{2} c_p^{*2}(c_m^* - c_p^*), \tag{41}$$

whereas the coefficient α in the expansion of c_m is not determined by the extreme curvatures. The coefficient β is

$$\beta = (-3c_p^{*2} c_p'^* + c_p'^* c_m^{*2} + \alpha^2 c_p^* + 2N c_p^* c_p'^* + L c_p'^*)/2 c_p^* c_m^* - 2c_p'^* \tag{42}$$

(ii) Possible limiting shapes

One can also pose the question of what are the shapes of a cell with given A and ΔA which have maximal volume. In a dimensionless representation, this means that we are looking for a shape with extremal relative volume v^* (Eq. 18) with the condition that the relative area a^* (Eq. 17) equals one and the relative area differ-

ence Δa^* (Eq. 19) equals Δa. We therefore study the functional

$$h = v^* - \tfrac{1}{4}\tilde{L}(a^* - 1) - \tfrac{1}{2}\tilde{N}(\Delta a^* - \Delta a) \tag{43}$$

The Euler-Lagrange minimization procedure leads, if we restrict ourselves to shapes which are smooth at the poles, to an algebraic equation for the curvature c_p

$$\tilde{N} c_p^2 + \tilde{L} c_p - 6 = 0\,, \tag{44}$$

which means that the curvature c_p is constant over the surface. From Eq. (20), we see that in such a case c_m is also constant and equal to c_p. We therefore conclude that the surface which corresponds to the solution of Eq. (44) is a sphere or a section of a sphere. As Eq. (44) has in general two different solutions, we conclude that the limiting shapes consist of spheres or of sections of spheres where only two different radii are allowed.

Let us analyse in more detail some simple limiting shapes

a) A simple possibility is, that a limiting shape consists of two spheres with different radii. By requiring that the relative area of the cell equals one and that the relative area difference equals Δa, one can determine the two relative radii $r_1 \geqq r_2$

$$r_1 = \tfrac{1}{2}\{\Delta a + [2 - (\Delta a)^2]^{1/2}\} \tag{45}$$

$$r_2 = \tfrac{1}{2}\{\Delta a - [2 - (\Delta a)^2]^{1/2}\}\,. \tag{46}$$

The maximum volume v_e is then given by

$$v_e = \tfrac{1}{2}\Delta a[3 - (\Delta a)^2]. \tag{47}$$

For $1 < \Delta a < 2^{1/2}$ the dependence $v_e(\Delta a)$ is shown in Fig. 1 (line no. 2) For $\Delta a = 2^{1/2}$ one obtains a limiting shape composed of two equal spheres. With decreasing Δa, one radius increases and the other decreases until at $\Delta a = 1$, one radius equals zero and only one sphere remains.

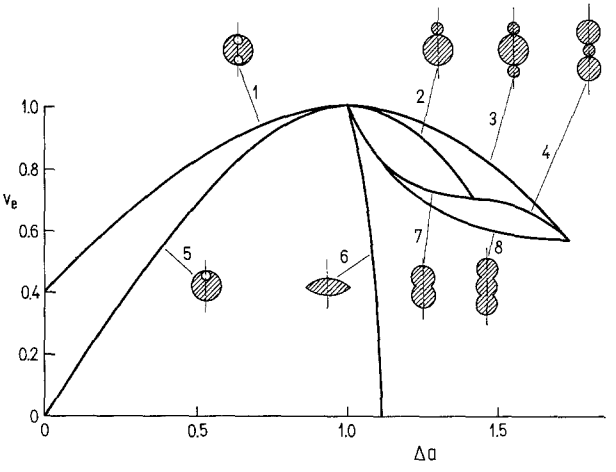

Fig. 1. Some extreme relative volumes (v_e) as a function of relative leaflet area difference (Δa), together with corresponding limiting shapes. Lines 2 and 5 are obtained from Eq. (47) and lines 6 and 7 from Eqs. (48) and (49)

For $0 < \Delta a < 1$, r_2 is negative and the corresponding shape is shown in Fig. 1 (line no. 5). By decreasing Δa, the internal vesicle increases up to $\Delta a = 0$ where its radius becomes equal to the radius of the cell.

b) Another simple possibility for the limiting shape is that it has a mirror plane symmetry and is composed of two equal sections of a sphere (Fig. 1, lines no. 6 and 7). In this case one obtains a parametrical expression for $v_e(\Delta a)$ as

$$v_e = \frac{1}{2^{1/2}} \sin(\phi/2) \cos^2(\phi/2)\,[3 + \mathrm{tg}^2(\phi/2)] \tag{48}$$

$$\Delta a = \frac{1}{2^{1/2}} \cos(\phi/2)\,[\pi/2 - \phi + 2\,\mathrm{tg}(\phi/2)] \tag{49}$$

The parameter ϕ here gives the angular magnitude of the section of the sphere. For $0 < \phi < \pi/2$ the sections are smaller than half of the sphere and these shapes correspond to line no. 6 in Fig. 1. For $\phi = \pi/2$ one obtains a single sphere ($\Delta a = 1$, $v_e = 1$), while for $\phi > \pi/2$ the sections are larger than half of a sphere (Fig. 1, line no. 7).

Figure 1 also shows some other examples of limiting shapes and dependencies of their relative volumes on the relative leaflet area difference.

Results

The general result of the preceding theory is all possible shapes and the corresponding membrane bending energies at any set of values of relative volume v and relative leaflet area dfference Δa. A more compact form of presenting this result is to introduce certain classes of shapes defined in the following way. A class of possible PV or RBC shapes constitutes the shapes which can be obtained in a continuous and derivable manner from a given shape at certain values of v and Δa, if v and Δa are continuously changed. As the previously performed analysis of limiting shapes suggests, the classes of shapes so defined may exist within certain parts of the $v/\Delta a$ diagram only.

In the present work we mainly consider the behavior of two low energy classes of PV or RBC shapes, the class of axisymmetrical shapes involving reflection symmetry with respect to the equatorial plane of the object, which includes discocyte shapes (designated *S* in the following), and the class of the axisymmetrical shapes without such symmetry, which includes cup shapes (designated *A*).

Firstly, the shapes of these two classes and the corresponding membrane bending energies are determined for an object with a given relative volume v and by varying the relative leaflet area difference Δa. Such calculations mimic the experimental situation in which, by physical or chemical means, the difference in

the leaflet areas is changed by keeping the volume of the object and its membrane area constant. For instance, the volume of giant PV remains practically constant during the observation of shape changes because of the relatively low water permeability of phospholipid membranes. The volume of RBC is osmotically regulated by processes which need not be affected by perturbations causing the Δa changes. The membrane area can be considered to be practically constant because the change in the area of one of the bilayer leaflets necessary to cause relevant shape changes is less than 1% of the total leaflet area (Beck 1978; Svetina et al. 1982). Figure 2 shows the dependence of the relative membrane bending energy on Δa for the value of relative cell volume $v = 0.6$ for classes S and A. In Fig. 3 are given examples of some of the corresponding shapes. Symmetrical discoidal shapes (class S) are shown within the interval $0.996 \leqq \Delta a \leqq 1.073$. The lower bound is a discocyte shape at which the two poles of the object come into contact. At values of $\Delta a < 0.996$ there is a finite amount of membrane in contact. The upper bound is the limiting shape resembling a bi-valved shell (see Fig. 1, line no. 6). In the interval $0.996 < \Delta a < 1.062$, the object has a discoid shape with the distance between the poles increasing with increasing Δa. At values $\Delta a > 1.062$ the object resembles an ellipsoid. The membrane bending energy has its smallest value at $\Delta a = 1.038$, where the shape is discocyte. As here $N = 2\partial w_b/\partial \Delta a = 0$ this is the shape which can be obtained by minimizing the membrane bending energy by taking into consideration only the constraints of constant membrane area and object volume. The present result thus confirms the results of Canham (1970).

In the interval $0.426 < \Delta a < 1.034$, there exist asymmetrical cup shapes (class A). The upper bound represents a shape belonging to the class of symmetrical discoidal shapes described above. At this value of Δa, the symmetrical shapes become unstable and are unstable below this value. The description of the nature of this instability is outside the scope of this paper and will be treated separately. The lower bound is the limiting spherical shape involving an inside spherical vesicle with an inside out oriented membrane (line no. 5 in Fig. 1). The series of shapes shown in Fig. 3 (designated by A) illustrates the dependence of these asymmetrical shapes on the value of Δa. Starting with $\Delta a = 1.034$ and decreasing Δa, the curvature at one of the poles increases whereas at the other pole, its value decreases. Below $\Delta a = 0.96$ only a single dimple is left. There is a special shape at $\Delta a = 0.78$ where new extrema in the function $f(z)$ appear. Below $\Delta a = 0.78$ the mouth of the cavity is closing at decreasing Δa and closes finally when the limiting shape is reached. The membrane bending energy of the asymmetrical shapes at $v = 0.6$ involves two extreme values with respect to

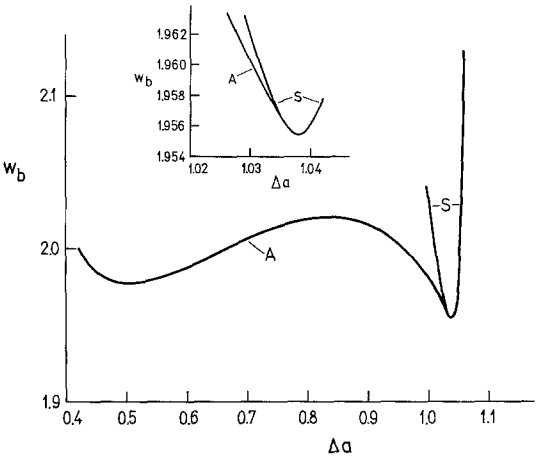

Fig. 2. The dependence of the relative membrane bending energy w_b on the relative leaflet area difference (Δa) for $v = 0.6$ and for S: the class of axisymmetrical shapes with equatorial mirror plane symmetry, which includes discocyte shapes (symmetrical discoidal shapes), and A: the class of axisymmetrical shapes with broken equatorial mirror plane symmetry, which includes cup shapes (asymmetrical cupped shapes). In the inset is shown an enlarged part of the diagram close to the minimum. It can be seen that the A-class continuously transforms into the S-class

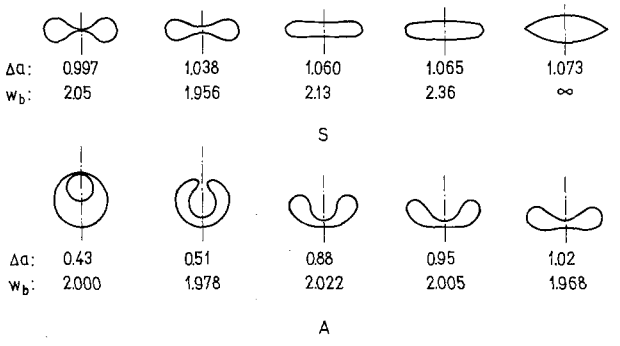

Fig. 3. Characteristic examples of symmetrical discoidal shapes (S) and asymmetrical cupped shapes (A) at relative volume $v = 0.6$. All shapes except the two limiting shapes (at $\Delta a = 1.073$ and $\Delta a = 0.43$) are obtained numerically by solving Eqs. (26)–(29) and (32). The corresponding relative leaflet area differences (Δa) and the relative membrane bending energies (w_b) are given

Δa changes (Fig. 2). At $\Delta a = 0.83$ there is a maximum and there is a minimum at $\Delta a = 0.51$. The limiting shape has the value $w_b = 2$, as expected for a general shape which is composed of two spheres.

The dependence of the relative membrane bending energy on Δa as presented in Fig. 2 shows how the system would behave if the constraint $\Delta a = \text{const.}$ were removed. If initially $\Delta a > 0.83$ an object would eventually become a discocyte with $\Delta a = 1.038$ whereas with the initial $\Delta a < 0.83$, an object would become a stomatocyte with $\Delta a = 0.51$. This tendency of the system is most clearly seen from the Δa dependence of the derivative $\partial w_b/\partial \Delta a$ (Fig. 4c). It is of interest to

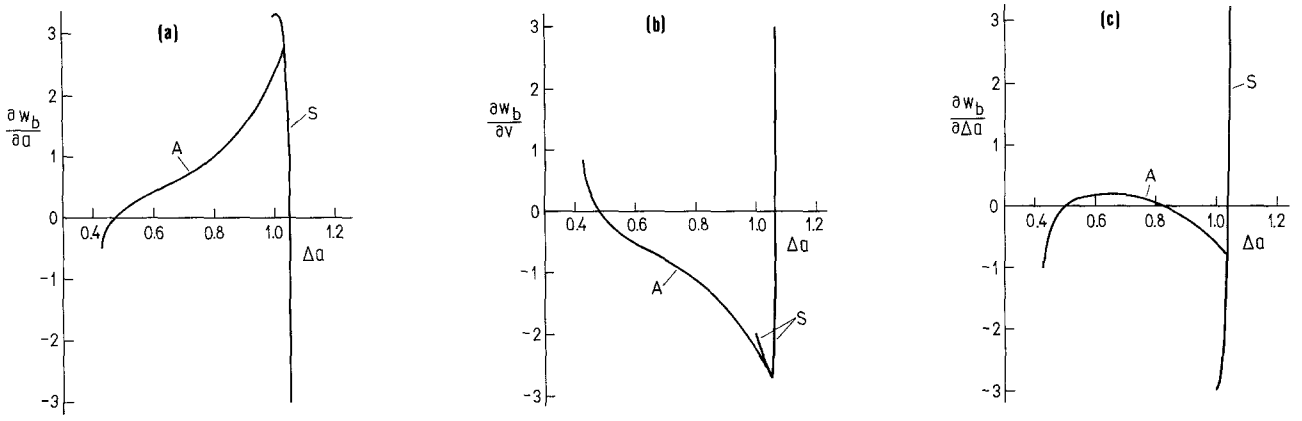

Fig. 4a–c. Partial derivatives of the relative membrane bending energy by relative membrane area (**a**), relative volume (**b**), and relative difference between the areas of the two bilayer leaflets (**c**) as functions of the relative difference between the areas of the two bilayer leaflets at $v = 0.6$. *S*: symmetrical discoidal shapes; *A*: asymmetrical cupped shapes

	$\frac{\partial w_b}{\partial \Delta a}$	$\frac{\partial w_b}{\partial a}$	$\frac{\partial w_b}{\partial v}$
I	< 0	< 0	> 0
II	< 0	> 0	> 0
III	< 0	> 0	< 0
IV	> 0	> 0	< 0
V	> 0	< 0	< 0
VI	> 0	< 0	> 0

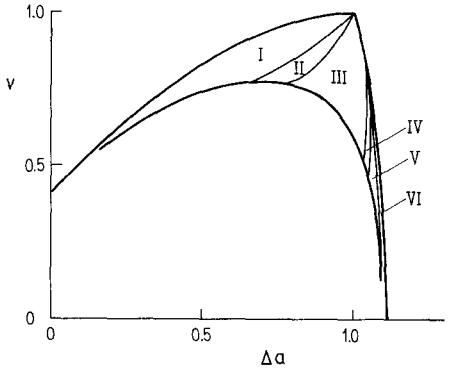

Fig. 5. Representation of the region in the $v/\Delta a$ diagram belonging to the class of symmetrical discoidal shapes (*bold lines*). The region is subdivided (*thin lines*) into parts with different signs of the partial derivatives of the membrane bending energy by membrane area, volume, and difference between the areas of the bilayer leaflets, as shown. Lines which divide these parts of the region are obtained by calculating shapes in which one of the Lagrange multipliers *L*, *M* or *N* is taken to be zero

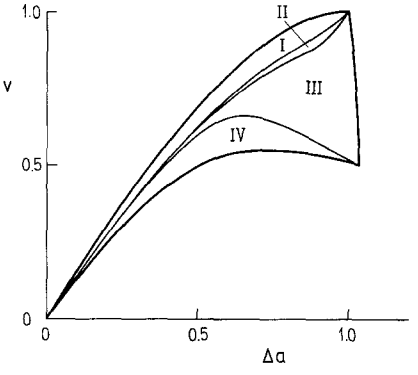

Fig. 6. Representation of the region in the $v/\Delta a$ diagram belonging to the class of asymmetrical cupped shapes (*bold lines*). The region is subdivided into parts (*thin lines*) as in Fig. 5

know the tendency of the system also for the case of the removal of other constraints. In Fig. 4 are therefore shown also the derivatives of the relative membrane bending energy with respect to relative area (a) and relative volume (b). An interesting observation made is that at Δa values close to the limiting shapes, $\partial w_b/\partial v$ is positive, which means that the tendency is to decrease the volume, whereas $\partial w_b/\partial a$ is negative and the membrane area tends to increase.

The generalization of the described behavior of the system to other relative volumes leads us to a more general characterization of the two classes of shapes described. Figures 5 and 6 show some properties of these classes. The treated symmetrical shapes which have a finite distance between the poles can only be realized at v and Δa values within certain boundaries (Fig. 5, bold lines). The upper boundary with respect to the Δa values are shapes resembling a bi-valved shell (Fig. 1, line no. 6). The lower boundary with respect to the Δa value is another limiting shape, a sphere involving two invaginated equal spheres (line no. 1 in Fig. 1). The third boundary line appearing in Fig. 5 represents shapes with the two poles touching each other. The area in the $v/\Delta a$ diagram belonging to the treated class of symmetrical shapes is still further divided by lines which correspond to the value zero for each of the three Lagrange multipliers (Fig. 5, thin lines). In the sections of the class so obtained, the partial derivatives of the total membrane bending energy have different combinations of signs, as given in Fig. 5. An analogous representation of the class of asymmetrical cupped shapes is given in Fig. 6. Here the bound-

ary of the class at lower values of Δa is the limiting shape involving a single invaginated sphere (Fig. 1, line no. 5). The upper boundary with respect to Δa values is the line at which the shapes become symmetrical. Also in this case the third boundary represents shapes with touching poles.

Discussion

Minimization of the membrane bending energy under the constraint of bilayer couple provides for a variety of PV and RBC shapes which depend on the values of the relative vesicle volume v and the relative leaflet area difference Δa. The shapes so obtained do not depend on the value of the membrane bending elastic constant. The result of the present analysis is various special properties of the system, in which the first to be discussed is the geometrical limitations imposed by the bilayer couple. If there is a shape corresponding to certain initial values of v and Δa, and either v continuously increases or Δa continuously increases or decreases, the process can in general be continued only up to a certain limit within the $v/\Delta a$ diagram. The shapes corresponding to these limits are compositions of sections of spheres in which only two sphere radii are possible. Shapes which are compositions of spheres are a common observation in experiments involving giant phospholipid vesicles (Sackmann et al. 1986). RBC vesiculation can also be considered as experimental support for the existence of limiting shapes. The usual result here is the occurrence of a spherical cell and a large number of small vesicles of about the same size. The vesicles obtained either have a normally oriented membrane or an inside out oriented membrane. The present analysis suggests that the right side out oriented vesicles are the ultimate result of the processes by which the leaflet area difference Δa increases, and that the inside out ones are the ultimate result of any procces by which the Δa decreases. It has been recently observed that agents which are known to modulate RBC shape do also influence the vesiculation behavior of the cells (Bütikofer et al. 1987) which is in accordance with the predictions of the present theory. However, in relating the present theory and the vesiculation processes it should be noted that the limiting shapes determined here still represent bodies with a connected surface. The transition from a certain limiting shape to a state of the system in which the vesicles are separated must involve mechanisms which are outside the scope of the present theoretical treatment.

Another interesting feature of the system studied is the existence of axisymmetrical shapes involving different symmetry properties. The present analysis indicates that discocytic and cupped RBC shapes are members of two different classes of possible shapes of the bilayer couple system. These two classes have a common line in the $v/\Delta a$ diagram which is an instability line of the symmetrical shapes.

Whereas the treatment of idealized PV and RBC systems in which the shape is assumed to correspond to the minimum membrane bending energy at constant volume, membrane area and difference between the areas of the two membrane leaflets provides a clear representation of the general features of the bilayer couple system, it is important also to visualize in what way these general features persist when additional real properties of the systems analyzed are taken into consideration. An example of such a property is the spontaneous curvature, which is expected to be nonzero if there is any asymmetry in the structure and composition of the two bilayer leaflets. The bending energy in this case is

$$W_{bc} = \tfrac{1}{2} K \int (C_1 + C_2 - C_0)^2 \, \mathrm{d}A^* . \tag{50}$$

Here C_0 is the spontaneous curvature which is the material property of the membrane. In a dimensionless formulation, the above bending energy can be expressed as

$$w_{bc} = w_b - c_0 \Delta a^* + \tfrac{1}{4} c_0^2 , \tag{51}$$

where $c_0 = C_0 R_s$ and R_s is given by Eq. (5).

It is easy to see that by minimizing the above bending energy at constant spontaneous curvature c_0 and at given values for relative volume, relative area and relative leaflet area difference ($\Delta a^* = \Delta a$) one obtains the same shapes as before, when only w_b was minimized, because the last two terms in Eq. (51) are constant. Because of these two terms, only the energy of the obtained shapes changes. Consequently, the Δa value at which the bending energy is at an extremum is changed. A positive c_0 shifts the minima to larger Δa values and maxima to smaller Δa values.

It is of interest to relate the present treatment of PV and RBC shapes to the work of Deuling and Helfrich (1976 a) and others (Jenkins 1977; Luke 1982; Peterson 1985). In these works the membrane bending energy (Eq. 50) is minimized under the constraints of constant volume and membrane area, leaving the leaflet area difference Δa free. This is the limiting case of the present treatment in which the constraint of constant leaflet area difference is removed and we can put $N = 0$, i.e. we look for the extrema of w_{bc} as a function of Δa at constant relative volume. Physically this case can be realized, for instance, by the flip-flop processes for phospholipid molecules.

In general, the extrema are obtained by minimizing expression (51) with respect to Δa

$$\frac{\mathrm{d}w_{bc}}{\mathrm{d}\Delta a} = \frac{\mathrm{d}w_b}{\mathrm{d}\Delta a} - c_0 = 0 \tag{52}$$

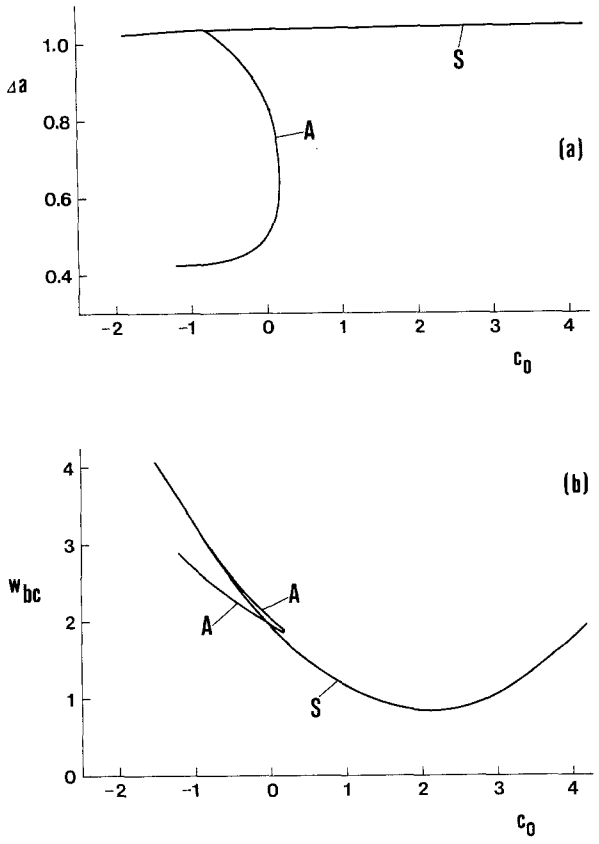

Fig. 7. a Relative leaflet area difference Δa corresponding to the extreme energy shapes is shown for $v = 0.6$ in dependence of the spontaneous curvature c_0 for the class of symmetrical discoidal shapes (S) and for the class of asymmetrical cupped shapes (A). **b** The corresponding dependences of the membrane bending energy on c_0

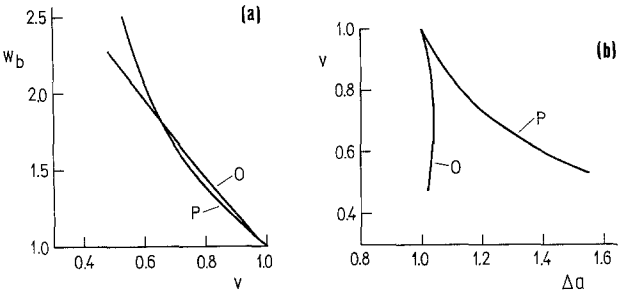

Fig. 8. a The minimum membrane bending energy as a function of the relative volume v shown for two classes of axisymmetrical shapes involving reflection symmetry. Shapes of the class designated O become oblate ellipsoids at v close to one whereas shapes of the class designated P become prolate ellipsoids at v close to one. All shapes are calculated by taking $N = 0$. **b** The lines in the $v/\Delta a$ diagram which correspond to these shapes are shown

For $v = 0.6$ the values of Δa and w_{bc} of the extremum shapes as a function of c_0 for treated classes of symmetrical and asymmetrical shapes are given in Fig. 7. Because of relation 52, Fig. 7 a which shows the dependence $\Delta a = \Delta a(c_0)$ is equal to the inverted Fig. 4 c. For the symmetrical class (S) the relative energy w_b has one single minimum (Fig. 2), which is relatively steep. The spontaneous curvature therefore changes the minimal Δa only slightly, shifting it to larger values for positive c_0. For the asymmetrical class (A) (Fig. 2), there are two extrema in $w_b(\Delta a)$: a minimum at $\Delta a = 0.51$ and a maximum at $\Delta a = 0.83$. The positive spontaneous curvature shifts the minimum to larger Δa and the maximum to smaller Δa, until they coalesce at $c_0 = 0.18$. Above $c_0 = 0.18$ the extreme asymmetric (A) solution no longer exists. For negative c_0, the minimum is shifted to smaller Δa and the maximum to larger Δa. It can be seen from Fig. 7 b that for $c_0 > -0.10$, the symmetric solution is stable, and that it transforms at $c_0 = -0.10$ discontinuously into an asymmetric solution with $\Delta a = 0.48$, which corresponds to an almost closed cup shape (Fig. 3). Within such a scheme for the discocyte-stomatocyte transition the usual stomatocytes are never stable.

For $v = 0.6$, which is believed to be the value corresponding to a normal RBC, and $c_0 = 0$, the absolute minimum of membrane bending energy corresponds to the discocyte shape (Figs. 2 and 3) which is the stable shape of a normal RBC. For larger volumes, i.e. in the limit $v \to 1$, this shape attains the form of an oblate ellipsoid and therefore this subclass of S can be denoted by O. The corresponding relative energies and relative area differences are shown in Fig. 8. There exists another class of symmetric shapes which become prolate ellipsoids for $v \to 1$ (class P). It can be seen from Fig. 8 a that for v close to one, the energy of the oblate solution is larger than the energy of the prolate shape, which is therefore stable. It has been suggested (Helfrich and Deuling 1975) that a large enough negative spontaneous curvature must exist for the oblate (i.e. discoid) shape to have a lower energy than the prolate one. It can be seen from Fig. 8 a that at $v = 0.6$ for $c_0 = 0$ the oblate shape has lower energy and no spontaneous curvature is needed to stabilize the discoid solution with respect to its prolate analogue. Figure 8 b shows the corresponding Δa values of the O and P subclasses. The two lines are considerably apart in the $v/\Delta a$ diagram, which means that a transformation from one shape to another involves a considerable transfer of the bilayer material from one membrane leaflet to another. Such a transformation is therefore quite improbable and it is thus possible for an object to be caught in the local minimum of membrane bending energy.

The presented treatment of the bilayer couple system is the limiting case of a more general approach in which the energies of other deformational modes of the membrane are taken into consideration. For the bilayer membrane in the liquid state there are two such

modes (Svetina et al. 1985), the stretching of the membrane

$$W_{str} = \tfrac{1}{2} K' (A - A_0)^2 / A_0 \tag{53}$$

and the relative stretching of the two membrane leaflets

$$W_{rstr} = \tfrac{1}{2} K'' (\Delta A - \Delta A_0)^2 \tag{54}$$

K' and K'' are the corresponding elastic constants. A_0 and ΔA_0 are equilibrium values of the average membrane area and the leaflet area difference, respectively, and A and ΔA are the corresponding values of the stretched state. The energy terms (53) and (54) can be included into the minimization procedure and the functional to be minimized then reads

$$G' = W_b + W_{str} + W_{rstr} - \mu(V^* - V). \tag{55}$$

It turns out that the Euler-Lagrange equations obtained are formally equivalent to the equations obtained by the minimization of the functional for G (Eq. 2) where, instead of Lagrange multipliers λ and v, we have

$$\lambda = -K'(A - A_0)/A_0 \tag{56}$$

$$v = -K''(\Delta A - \Delta A_0), \tag{57}$$

In order to predict shapes within such a generalization it is necessary to know the relative magnitudes of the elastic constants involved. It is assumed that it is much easier to bend the membrane than either to stretch it or to stretch the two membrane leaflets relatively, therefore the shapes obtained for a flaccid vesicle are not expected to differ appreciably from the shapes calculated on the basis of the theory presented in this work. The inclusion of stretching and relative stretching terms gains in importance when the shapes are close to the limiting shapes where vesicles are loosing their flaccidness. The study of the system under such conditions is also outside the scope of the present treatment.

The bilayer couple concept is not necessarily applicable to the shape problems of the RBC because this cell has, in addition to the two leaflets of the bilayer part of the membrane, also a network of cytoskeletal proteins. Experiments suggest that both parts of the membrane are involved in RBC shape formation. A possible approach to include the cytoskeletal proteins into the study of RBC shape formation and transformations is to consider the RBC membrane as a system of three layers which are free to move relative to one another but are in contact. The analysis of the mechanical properties of such a trilayer system (Svetina et al. 1988) shows that its elastic energy can be expressed as the sum of exactly the same deformational modes as the bilayer system, i.e. the bending, stretching and relative stretching terms. However, the meaning of the parameters is not so obvious as in the bilayer case. For instance, the parameters of the relative stretching term, K'' and ΔA_0 (Eq. 57), depend in a definite manner on the areas and stretching constants of all three composite layers, and the distances between their neutral surfaces. In conclusion, such an analysis implies that the bilayer couple concept is also applicable, at least under specific conditions, in the case of RBC shape transformations, only care must be taken about the actual meaning of the parameter ΔA_0.

The present studies lead to a general conclusion that the understanding of PV and RBC shape formation must be achieved at two separate levels. At the macroscopic level, the vesicle or cell shape is formed such that it corresponds to the minimum value of the elastic energy of the membrane. The parameters involved are the areas of the layers and their stretching and bending constants if there are three or more layers, and only the difference in the areas of the two leaflets in the case of the bilayer. At the microscopic level, there are different physical and chemical processes which regulate the magnitudes of these areas. It is important to realize that it is not the details of these processes but only their final result which determines the PV or RBC shape.

Acknowledgement. The authors thank Drs. W. Helfrich and Ou-Yang Zhong-can for the remark regarding the solution of the variational problem, Eq. (43).

References

Beck JS (1978) Relations between membrane monolayers in some red cell shape transformations. J Theor Biol 75: 487–501

Bütikofer P, Brodbeck U, Ott P (1987) Modulation of erythrocyte vesiculation by amphiphilic drugs. Biochim Biophys Acta 901:291–295

Canham PB (1970) The minimum energy of bending as a possible explanation of the biconcave shape of the human red blood cell. J Theor Biol 26:61–81

Deuling HJ, Helfrich W (1976a) The curvature elasticity of fluid membranes: A catalogue of vesicle shapes. J Phys (Paris) 37:1335–1345

Deuling HJ, Helfrich W (1976b) Red blood cell shapes as explained on the basis of curvature elasticity. Biophys J 16: 861–868

Deuticke B (1968) Transformation and restoration of biconcave shape of human erythrocytes induced by amphiphilic agents and changes of ionic environment. Biochim Biophys Acta 163:494–500

Evans EA (1974) Bending resistance and chemically induced moments in membrane bilayers. Biophys J 14:923–931

Evans EA (1980) Minimum energy analysis of membrane deformation applied to pipet aspiration and surface adhesion of red blood cells. Biophys J 30:265–284

Evans EA, Skalak R (1980) Mechanics and thermodynamics of biomembranes. CRC Press, Boca Raton, FL

Helfrich W, Deuling HJ (1975) Some theoretical shapes of red blood cells. J. Phys (Paris) Colloq 36:327–329

Hochmuth RM, Waugh RE (1987) Erythrocyte membrane elasticity and viscosity. Annu Rev Physiol 49:209–219

Jenkins JT (1977) Static equilibrium configurations of a model red blood cell. J Math Biol 4:149–169

Luke JC (1982) A method for the calculation of vesicle shapes. SIAM J Appl Math 42:333–345

Luke JC, Kaplan JI (1979) On theoretical shapes of bilipid vesicles under conditions of increasing membrane area. Biophys J 25:107–111

Peterson MA (1985) An instability of the red blood cell shape. J Appl Phys 57:1739–1742

Sackmann E, Duwe H-P, Engelhardt H (1986) Membrane bending elasticity and its role for shape fluctuations and shape transformations of cells and vesicles. Faraday Discuss Chem Soc 81:281–294

Sheetz MP, Singer SJ (1974) Biological membranes as bilayer couples. A mechanism of drug-erythrocyte interactions. Proc Natl Acad Sci USA 72:4457–4461

Svetina S, Žekš B (1983) Bilayer couple hypothesis of red cell shape transformations and osmotic hemolysis. Biomed Biochim Acta 42:86–90

Svetina S, Žekš B (1984) Red cell membrane properties and the bilayer couple hypothesis of red cell shape transformations. In: Tomicki B, Kuczera J, Przestalski S (eds) Biophysics of membrane transport, part II. Agricultural University Wroclaw, pp 107–126

Svetina S, Žekš B (1985) Bilayer couple as a possible mechanism of biological shape formation. Biomed Biochim Acta 44: 979–986

Svetina S, Ottova-Leitmannova A, Glaser R (1982) Membrane bending energy in relation to bilayer couples concept of red blood cell shape transformations. J Theor Biol 94:13–23

Svetina S, Brumen M, Žekš B (1985) Lipid bilayer elasticity and the bilayer couple interpretation of red cell shape transformations and lysis. Stud Biophys 110:177–184

Svetina S, Brumen M, Žekš B (1988) The role of the membrane elastic properties and cell volume in the formation of red blood cell shapes. In: Benga Gh, Tager JM (eds) Biomembranes: basic and medical research. Springer, Berlin Heidelberg New York, pp 177–187

Zarda PR, Chien S, Skalak R (1977) Elastic deformations of red blood cells. J Biomech 10:211–221